Emil P. Kartalov[1,2]
David H. Lin[2]
David T. Lee[2]
William F. Anderson[3]
Clive R. Taylor[1]
Axel Scherer[2]

[1]Department of Pathology, Keck School of Medicine, University of Southern California, Los Angeles, CA, USA
[2]Electrical Engineering Department, California Institute of Technology, Pasadena, CA, USA
[3]Department of Biochemistry, Keck School of Medicine, University of Southern California, Los Angeles, CA, USA

Received May 13, 2008
Revised June 19, 2008
Accepted June 23, 2008

Research Article

Internally calibrated quantification of protein analytes in human serum by fluorescence immunoassays in disposable elastomeric microfluidic devices

Herein we report on reliable reproducible quantification of protein analytes in human serum by fluorescence sandwich immunoassays in disposable PDMS microfluidic chips. The system requires 1000 times less sample than typical clinical blood tests and is specifically shown to measure ferritin down to 250 pM in human serum. The in-built calibration method of spiking the serum with known concentrations of commercially available antigen avoids common sources of error and improves the reliability of the test results. The reported microfluidic system is an important new tool for fundamental scientific research, offering sensitive immunoassay measurements in small but complex biosamples. The system is also a further step towards comprehensive affordable ''point-of-care'' biomedical diagnostics.

Keywords:
Diagnostics / Fluorescence / Immunoassay / Microfluidic / Serum
DOI 10.1002/elps.200800297

1 Introduction

The ongoing revolution in biological sciences has generated high hopes for the advent of true personalized/preventive medicine. While the necessary biological tools are being developed at a fast pace, it has become clear that their cost, operation, and manufacturability are equally challenging issues that must be solved before the new methods can enter widespread use in medical practice. In the particular case of diagnostics, decentralized 'near-patient' or 'point-of-care' testing [1] has striven to provide fast quantitative results at the bedside or in the clinic, thereby decreasing hospital stays, eliminating transportation and administrative expenses, and decreasing errors from mishandling and miscommunication. While a few portable systems [1, 2] have been developed (*e.g.* the now commonplace glucometer), the enormous potential for decentralized testing remains untapped as the vast majority of medical diagnostics is still conducted in clinical labs using large equipment [2].

A way for ubiquitous ''near-patient'' and ''point-of-care'' testing to reach fruition is for the current biological techniques to be reduced from the macro- to the micro-scale, preferably in multi-analyte high-throughput handheld devices. In particular, reducing immunoassays to microfluidic scales has been extensively explored in recent years. Many approaches have been proposed, involving glass [3–10], titanium dioxide [8], silicon [11–15], silicone [11, 16–31], silicon nitride [32], poly(methylmethacrylate) [33], polyurethane [34], mylar [35], polycarbonate [36], polyolefin [37], ethylenediamine film [38], compact discs [39], flow cells [40], and screen-printed chips [41]. These devices have striven to provide a list of the desirable qualities: (i) capability to measure multiple antigens and samples *per* device, (ii) industrially feasible fabrication, (iii) parsimony of sample and reagents, (iv) adequate sensitivity and specificity, and (v) adequate reliability and reproducibility.

We previously reported on a high-throughput multi-antigen microfluidic system quantifying four protein analytes at their clinically relevant levels [42]. However, those preliminary results were limited to working with simple buffer solutions and thus the important question remained if the system would be at all usable with complex biological media, such as human serum, plasma, cerebrospinal fluid, saliva, *etc.* The goal of the presented work is to address this question experimentally.

Herein we report on the successful reproducible quantification of protein analytes in human serum by fluorescence immunoassays in complex elastomeric microfluidic devices. The results demonstrate reproducible agreement with the values obtained for the same samples in standard clinical measurements in a hospital reference laboratory. The tech-

Correspondence: Professor Emil P. Kartalov, 2011 Zonal Avenue, HMR 301A, Los Angeles, CA 90089-9092, USA
E-mail: kartalov@usc.edu
Fax: +1-323-442-3212

Abbreviations: CRP, c-reactive protein; **DB,** derivatization buffer input; **DE1–5,** derivatization exhaust; **SB,** samples' buffer input; **SE1–6,** samples' exhaust

nique offers improved reliability by decreased susceptibility to measurement errors, through the use of an in-built calibration based on spiking the sample with known concentrations of commercially available antigens. The system is shown to quantify protein analytes in human serum down to 250 pM concentration. Furthermore, the maturity of the underlying technology [43] allows for future integration of multiple samples and multiple antigens within the same device for measurement under the presented human serum technique, thereby bringing the state of the art closer to the desired goal of ubiquitous affordable decentralized protein-based biomedical diagnostics using fingerpricks. Finally, sample economy makes our system ideally suited for applications where sample is scarce, *e.g.* with cerebrospinal fluid and pediatric serum, thereby enabling potentially impactful fundamental biomedical research.

2 Materials and methods

2.1 Fabrication, reagents, and experimental setup

Mold and chip fabrication and the experimental setup are the same as in the preliminary work [42]. Fresh resupplies of the same commercial reagents were utilized. The size of the microfluidic chip was reduced to 60 chambers (six sample coliseums in five test lanes, with two chambers *per* coliseum), while the chamber size was allowed to vary among test lanes (Fig. 1).

2.2 Device architecture

In sandwich immunoassays, a monoclonal antibody, specific to the target analyte (antigen), is bound to a surface. Next, the sample is put in contact with that surface, whereby the antibody captures the contained antigen. Then a labeled polyclonal antibody attaches to the antigen. The label (*e.g.* a linked enzyme creating fluorescent product or a fluorophore bound to the polyclonal antibody) generates a signal that is compared with a standard to quantify the captured antigen.

Our chips (Fig. 1A) multiplex this scheme using micromechanical valves [44] that direct the pressure-driven reagent flow as desired along a network of 10-μm tall, 100-μm wide microchannels (Fig. 1B). The ''four-way'' valving at each intersection in the test matrix forms a capture microchamber, within which the sandwich immunoassay is completed for a particular sample-test combination. Figure 1C shows a section of the array of the fluorescence spots generated in a typical experiment.

Channel resistances of test lanes were made approximately equal by adding length to the most direct route from source to exhaust, as exemplified by the zigzags in lanes 2, 3, and 4 (Fig. 1B). In addition, the lanes with smaller chambers were designed with wider channel segments connecting the chambers (Fig. 1B zoom-in), so that the total fluidic resistances of the matrix lanes were kept approximately the same. That feature helped avoid lane bias, as different lane resistances at the same pressure would have generated different throughputs and thus varying doses across the test matrix.

The sizes of the capture chambers were varied as an additional lever of control in configuring the dynamic range of the system. Intersection sizes of 20×20, 60×60, and 100×100 μm were utilized (Fig. 1B and C). The hypothesis was that larger area would allow the capture of more analyte before reaching surface saturation and thus would handle samples of high concentration of analyte, while smaller areas would concentrate the surface signal from a rare sample for high-sensitivity measurements.

2.3 Basic measurement scheme

In typical device operation, monoclonal antibodies flow from derivatization inputs (D1–5) to derivatization exhausts (DE1–5) in Fig. 1B. The antibodies covalently bond to the epoxide floor of the microchannels, producing the first layer of the immunoassay. A buffer feed (Tris 10 mM, 0.1% BSA) from derivatization buffer input (DB) to DE1–5 removes unbound excess protein and passivates any unreacted epoxide moieties that would otherwise produce background by binding protein in later feeds. Next, an identical buffer flows from samples' buffer input (SB) to samples' exhausts (SE1–6) to passivate the rest of the microchannels. The contained BSA passivates potential non-specific attachment sites on the elastomer walls as well.

As samples flow in parallel from S1–6 (samples' inputs) to SE1–6, each sample fills a corresponding pair of microchannels. When the appropriate valves are closed, each such pair forms a circular path (a coliseum [42]), which traps 10 nL of the respective sample. Then an array of peristaltic micropumps [44] drives each trapped volume around its coliseum with a lap time of 20 s. Within each coliseum, each antigen is captured in its respective microchamber, as determined by the first layer of the immunoassay. The same sample is allowed to run multiple laps to maximize extraction of the antigen from the sample.

After harvesting, buffer from SB to SE1–6 flushes out the sample volume. Parallel feeds of biotinylated antibodies from A1–5 (antibody inputs) to DE1–5 build up the third layers of the immunoassay in each microchamber. Buffer from DB to DE1–5 removes unattached antibody. Fluorescently labeled streptavidin in PBS buffer flows from SA (StreptAvidin input) to DE1–5. Buffer from DB to DE1–5 removes unattached excess. Then all valves are closed and fluorescence detection is conducted at each microchamber using an inverted optical microscope and an inexpensive cooled CCD camera. The fluorescence signal is integrated over the chamber area and then lessened by the off-channel background signal normalized for area, to produce the net fluorescence signal from the immunoassay

spot. That result is correlated with the fed analyte concentration [42].

2.4 Advanced measurement scheme – internal recalibration

In human serum measurements, we further improved on the above basic scheme. Instead of having multiple samples in the same chip, we aliquoted the serum sample and spiked each aliquot with varying known concentrations of a commercially available antigen analogous to the endogenous human analyte we wished to measure. These derivative samples were then fed into the chip in parallel together with a negative control sample containing PBS buffer with 0.1% BSA.

Then fluorescence signals from each image were obtained as described in Section 2.3. The values for the serum samples were then lessened by the negative-control value, to subtract the contribution from potential non-specific attachment of antibodies and fluorescence probes. The resulting net fluorescence signals were plotted as a function of spike concentration to produce a calibration curve. Under suitably chosen feed conditions that curve would be close to a straight line. The zero-spike value was divided by the slope of the linear fit to yield the endogenous analyte concentration.

This internal recalibration scheme has important advantages over its alternatives as it cancels out the influence of drift factors such as variations in reagent activity, surface chemistry quality, and device fabrication conditions. By comparison, a one-time calibration to be used with subsequent single-point measurements would be susceptible to these factors, while a non-serum calibration (*e.g.* by using spiked buffer solutions) would not take into account the endogenous conditions inside the real biosample.

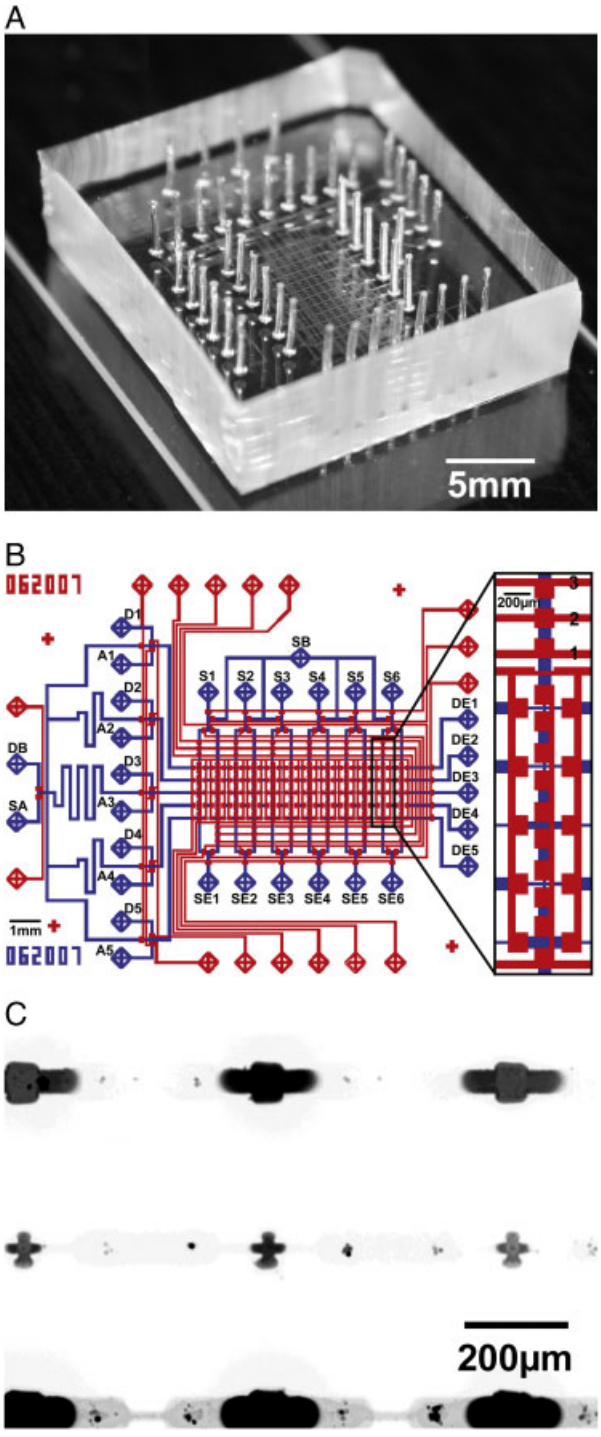

Figure 1. (A) Microfluidic immunoassay chip. A 60-chamber PDMS chip bound to a 1-in.-wide epoxide slide was used for the experiments. The vertical cylinders are input ports for reagents and control pressure. The microchannel test matrix is visible in the middle. (B) Architectural diagram of the entire chip. Control channels (red) convey pressure to open and close microvalves, which steer reagents along flow channels (blue). Each intersection of flow channels in the central test matrix forms a microchamber where an immunoassay is constructed. Monoclonal antibodies flowing from inputs D1–5 to exhausts DE1–5 bind to the epoxide coating of the microchannel floor. Buffer flushes from input DB to exhausts DE1–5 and from input SB to exhausts SE1–6 passivate remaining epoxide groups. Samples are fed in parallel from inputs S1–6 to exhausts SE1–6 and pumped along closed circular 10-nL paths through the capture microchambers. Biotinylated polyclonal antibodies fed from inputs A1–5 to exhausts DE1–5 complete the sandwich immunoassays. Labeled streptavidin fed from input SA to exhausts DE1–5 binds to the biotinylated antibody. The detected fluorescence signal quantifies the captured antigen. (B, inset) Architectural diagram of a test column. Vertical and horizontal comb-like valve arrays enclose individual chambers. Each coliseum contains two test columns and each test column contains five chambers. Valve arrays 1, 2, and 3 pump the sample in a circle along each coliseum (*e.g.* here upward for actuation order 1,2,3) with a lap time of 20 s. (C) Fluorescence immunoassay spots. Strong fluorescence signal emanates from the capture chambers when the sought antigen is present in the sample and the sandwich immunoassays are properly completed. Darker color corresponds to higher fluorescence intensity.

2.5 Accounting for variability

In this work, the main question we set out to answer was: ''Would our microfluidic immunoassay system function reliably with complex biological samples?'' The primary obstacle in such functioning would be loss of specificity and excessive noise, *e.g.* due to overwhelming non-specific attachment from the rich selection of proteins within the same serum sample and/or from the biological variability among patients.

One possible approach was to quantify many patients individually, both by chip and by clinical means, and then compare the results produced by the two methods. However, we realized that in terms of required time and resources it was more efficient to combine the serum samples of ten randomly chosen patients and perform measurements on the combined sample. Any interfering protein would therefore be present at only a $10\times$ dilution and thus would still be quite well accounted for, *e.g.* if it were to cause a technical problem with the measurements, especially at low endogenous analyte concentrations. Simultaneously, the number of independent measurements necessary for proof of principle of the system was drastically reduced. Thus, the described measurements were conducted on the compound serum sample.

2.6 Safety considerations

Standard safety precautions were observed in working with the human serum samples to prevent the transmission of potentially present human pathogens. Hand and eye protections were employed at all times, while the devices, connective tubing, and pipette tips used in sample preparation and measurement were discarded into biohazard bins and subsequently incinerated.

3 Results

3.1 Quantifications of protein analytes in human serum

We used the internal recalibration scheme to quantify the endogenous concentrations of ferritin, prostate-specific antigen, thyroglobulin, c-reactive protein (CRP), and vascular endothelial growth factor, within the compound serum sample. Best results were obtained with CRP and ferritin, most likely because their medically ''normal'' concentrations are highest among the selected analytes (1.2 mg/dL, 110 nM for CRP; 30–300 ng/mL, 350–3500 pM for ferritin). Vascular endothelial growth factor (2500 pg/mL, 96 pM ''normally'') and prostate-specific antigen (4 ng/mL, 130 pM for a ''normal'' male) produced measurable signals; however, the related uncertainties were high and thus the resulting linear fits were unreliable. Thyroglobulin (''normal range'' of 5–50 ng/mL or 42–420 pM) appeared essentially undetectable with the antibodies we had.

Consequently, we selected ferritin for further tests, since (among the chosen five analytes) ferritin had the lowest endogenous concentration that could still be quantified reliably with the available antibodies. In this way, we could minimize the limitations imposed by imperfect antibodies and thus best assess the intrinsic performance of the system itself, which was the ultimate goal of this study. We conducted a series of experiments to optimize the experimental parameters (*e.g.* feed pressure, feed duration, pump duration and frequency, spike concentrations, and photoexposure) to adjust the dynamic range of the system so that the calibration curves were as close to linear as possible.

A particular example of a ferritin calibration result is shown in Fig. 2. Of the six available coliseums, one was used for a negative control (PBS buffer, 0.1% BSA) to estimate non-specific attachment, one was used with pure (unspiked) serum, and the other four with the same serum but spiked to respective concentrations of 0.3, 0.6, 1, and 3 nM of commercially available antigen. The specifics of this experiment included two capture cycles, each comprising a 30-s sample feed and a 5-min circular pumping. A fluorescence image of each capture chamber was taken with a 4-s photoexposure.

The resulting calibration curve (Fig. 2) was used to estimate the endogenous ferritin concentration, yielding a value of 254 ± 35 pM. By comparison, the independent clinical measurement (obtained through Roche Elecsys 2010 in the USC Reference Laboratory) had yielded 198 pM for the same serum sample. Thus, in this case, our microfluidic device measured 28% higher concentration than the commercial macrosystem.

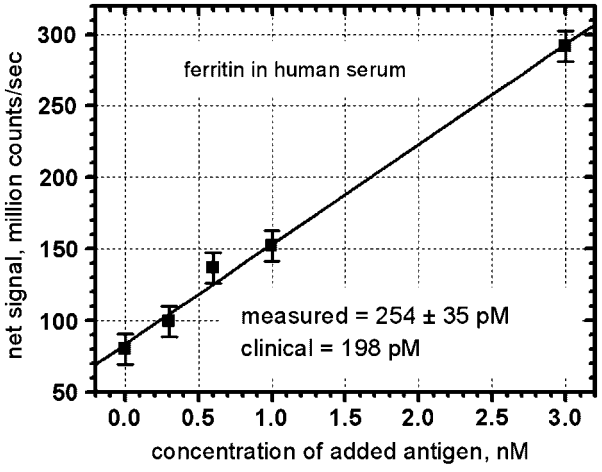

Figure 2. Quantification of ferritin in human serum. The serum sample was spiked with known concentrations of commercially available ferritin. The endogenous ferritin concentration is calculated from the slope of the linear fit and the zero-spike value. Here, the chip result was 254 ± 35 pM, while the clinical result was 198 pM.

3.2 Reproducibility and reliability measurements

We conducted 36 analogous measurements on the same serum sample to assess the degree of reliability and reproducibility of the obtained results. For each serum measurement, the estimated value of ferritin concentration was divided by the clinically measured value to produce a ratio parameter *R*. Figure 3A presents the compiled data as a scatter plot of the values of *R* for the 36 experiments we conducted. Figure 3B presents the same data in the form of a histogram. A normal fit to the histogram distribution yielded a mean of 1.46 with a standard deviation of 0.54.

We observed no visible difference or systematic clustering among subsets of measurements. The results showed agreement and reproducibility across different test lanes in the same device as well as across different devices, thereby demonstrating the overall reproducibility and reliability of the system. We believe the chief contributor to the observed quality is the in-built recalibration scheme.

4 Discussion

In designing the research work for this project, we chose to concentrate on proof-of-principle for this system for work with human serum samples, instead of a full clinical instrument validation, *e.g.* as done industrially and according to Food and Drug Administration regulations. Since we chose the former, we could limit ourselves to the described scheme of combining the serum samples of multiple patients into a compound sample and quantifying that sample in multiple experiments. Obviously, the scope and requirements for the latter would have been much broader, including systematic quantifications of a large number of separately measured patients, *e.g.* to study and account for the effects of biological variability on the system's functionality. However, such an undertaking is so broad and expensive that it was clearly beyond our means. As a result, we concentrated on the smaller scope, namely, the scientific proof-of-principle for the system for work with human serum. Undoubtedly, given sufficient resources, further work can be undertaken to accomplish the clinical validation as well, *e.g.* in an industrial setting.

The observed difference between the measured absolute values by standard clinical systems and our chips (Fig. 3) is very intriguing. However, even as is, the system can be used to quantify analytes, so long as the appropriate conversion is applied to make the results interpretable within the context of the current clinical diagnostic tables.

In medical practice, ''normal'' values are obtained by statistics on the same type of measurement done in the same way on a very large number of patients. The resulting distribution yields confidence intervals, which are then used to define ''the normal value''. Subsequently, any clinically measured value is compared with the ''normal''. That comparison determines if the analyte is over-expressed or under-expressed in the particular patient, who is then diagnosed accordingly.

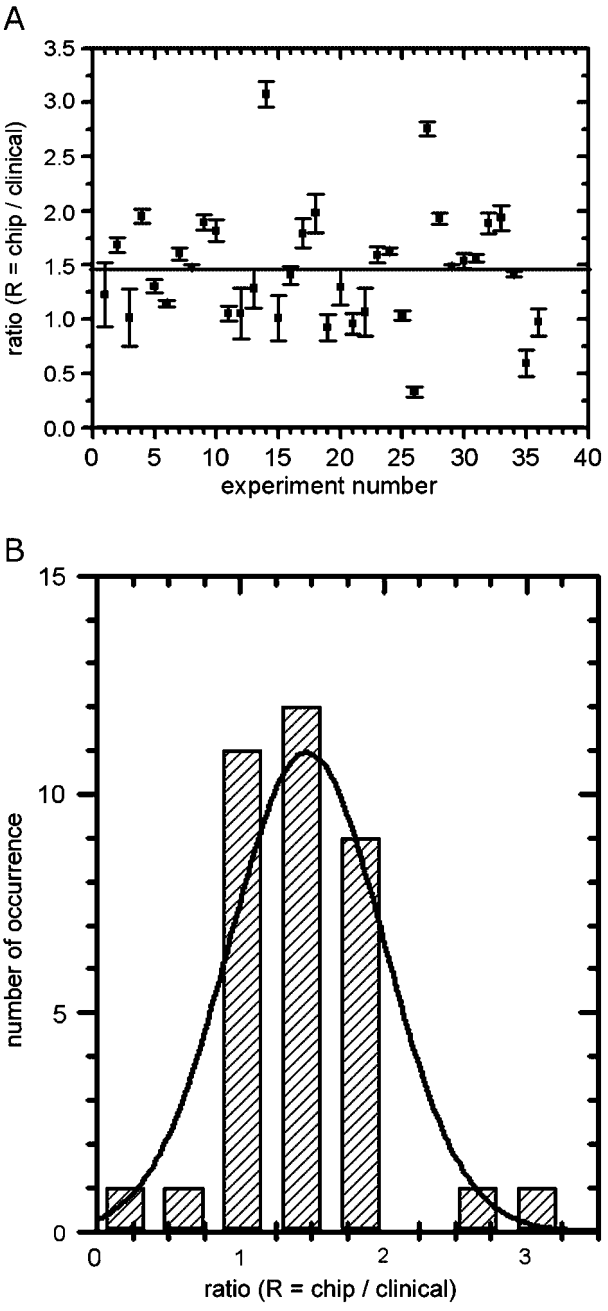

Figure 3. Instrumental statistics. The results of 36 analogous measurements of ferritin in the same human serum sample are presented as a scatter plot (A) and a histogram (B). No systematic clustering among subsets of measurements was observed. The results showed agreement and reproducibility across different test lanes in the same chip as well as across different chips, thereby attesting to the overall reproducibility and reliability of the system.

Consequently, in biomedical measurements, metrological consistency and precision are far more important than the accuracy of the absolute value. In fact, there would be no practical difference so long as all measurements are ''inac-

curate in a consistent way''. From that perspective, the mean value offset we observe is inconsequential in practical terms. Hence, in principle our system is immediately usable with the old tables of ''normal values'', by a simple arithmetic adjustment.

Thus, the critical parameter in judging the quality of our system is the consistency of measurements, as quantified by the standard deviation of the histogram fit. A standard deviation of 107 pM (0.54×198 pM) sounds quite usable as the ''normal'' clinical ferritin range is 350–3500 pM.

In comparison with other miniaturized devices, our system is one of the few to have demonstrated the capability of working with realistic biomedical samples. While it is prudent and useful to test and debug emerging systems with buffer solutions as a preliminary step, the ultimate challenge is to produce meaningful results with real biosamples such as human serum, plasma, cerebrospinal fluid, urine, saliva, *etc.* With that requirement in place, the selection of demonstrated devices becomes far more limited [11, 21, 22, 25, 28, 29, 32, 36–38, 40]. Among them, our system is the apparent leader with quantitative sensitivity to as low as 250 pM antigen in human serum, with one exception [25] utilizing surface plasmon resonance. However, surface plasmon resonance is expensive and difficult to parallelize and miniaturize. Also, Mulvaney *et al.* [40] have reported on a very promising technique using fluidic force discrimination and microbeads, but their biosample results are currently limited to qualitative detection only.

To our knowledge, among the systems working with realistic biological samples, ours and Linder's [28] are the only ones utilizing an internal recalibration as part of every measurement. The latter makes use of a second fluorophore as an internal standard. However, multiple fluorophore measurements require a more complex and expensive optical system and thus increase cost and impede miniaturization. Our system achieves recalibration and much higher sensitivity, while still working with a single type of fluorophore.

Our system is also an improvement over the current large expensive macrofluidic robotic systems in clinical practice, as our disposable chips are less expensive and practically use a few microliters of sample. By comparison, commercial robots generally require several milliliters for multiple tests and thus necessitate a phlebotomist taking blood from the vein of the patient. In principle, our devices can form the core of affordable decentralized portable systems for point-of-care diagnostics that replace phlebotomy with fingerpricks, make tests more accessible to pediatric patients, significantly speed up the test turnover time, and decrease overall medical costs [2]. The in-built recalibration is an additional major advantage, as it eliminates certain sources of error and thus makes the results more reliable.

These advantages are achieved at the price of higher complexity of microfluidic devices. Thankfully, the maturity of microfluidic technology [43] fundamentally allows for reliable operation of such devices, which accommodate the necessary functionalities and their respective architectures. More specifically, each immunoassay measurement under our scheme requires six subsamples. These are currently prepared off-chip but in a future embodiment can and will be split and spiked on-chip to pre-determined concentrations through microfluidic metering [45]. The additional complexity would not lead to undue increase in real estate, especially nowadays with the advent of microfluidic vias [46].

The engineering of the overall system and the low cost *per* device combine to offer the very important advantage of disposability. Disposability circumvents a host of problems, such as carryover contamination, cross-patient errors, biohazard issues, and maintenance downtimes due to sequential processing [2]. Getting ready for a new measurement is as simple as discarding one chip and replacing it with a new one within the same control and detection unit. This architecture is optimal in terms of cost and performance, and thus stands the best chance of adoption in biomedical practice.

That adoption would be further facilitated by overall system miniaturization. The latter would benefit from the development of miniaturized on-chip pneumatic actuation as well as a miniaturized detection system, *e.g.* based on an electrochemical signal, to replace the currently used fluorescence microscope. With such further advances, the promise of point-of-care biomedical diagnostics would become a reality for immunoassay-based measurements. What we demonstrated herein is the microfluidic immunoassay core of this future system and its ability to quantify protein analytes in human serum.

In conclusion, the presented work demonstrates the reduction of fluorescence immunoassays in human serum to a microfluidic format featuring a host of advantages, such as high sensitivity, parallelism, parsimony of sample, disposability, and miniaturizability. The demonstrated system is an important technological development for consequent immunoassay applications in scientific research and ''point-of-care'' biomedical diagnostics.

The authors thank Christina Morales and Anna Chetverikova of the Caltech Microfluidic Foundry for their help with device fabrication. The authors also thank Avril Cunningham of the USC Leavy Library for her help with the reference material. Financial support for this work was provided by NIH Grants 1K99EB007151 and 1RO1HG002644 and the Caltech SURF Program.

The authors have declared no conflict of interest.

5 References

[1] Gilbert, H. C., Szokol, J. W., *Int. Anesthesiol. Clin.* 2004, *42*, 73–94.

[2] Kartalov, E. P., *J. In-Vitro Diagn. Technol.* 2006.

[3] Wang, J., Ibanez, A., Chatrathi, M. P., Escarpa, A., *Anal. Chem.* 2001, *73*, 5323–5327.

[4] Fruetel, J. A., Renzi, R. F., VanderNoot, V. A., Stamps, J. *et al.*, *Electrophoresis* 2005, *26*, 1144–1154.

[5] Angenendt, P., Glockler, J., Konthur, Z., Lehrach, H., Cahill, D. J., *Anal. Chem.* 2003, *75*, 4368–4372.

[6] Delehanty, J. B., Ligler, F. S., *Anal. Chem.* 2002, *74*, 5681–5687.

[7] Sapsford, K. E., Charles, P. T., Patterson, C. H., Jr., Ligler, F. S., *Anal. Chem.* 2002, *74*, 1061–1068.

[8] Sydor, J. R., Scalf, M., Sideris, S., Mao, G. D. *et al.*, *Anal. Chem.* 2003, *75*, 6163–6170.

[9] Holmes, D., She, J. K., Roach, P. L., Morgan, H., *Lab Chip* 2007, *7*, 1048–1056.

[10] Herr, A. E., Throckmorton, D. J., Davenport, A. A., Singh, A. K., *Anal. Chem.* 2005, *77*, 585–590.

[11] Wolf, M., Juncker, D., Michel, B., Hunziker, P., Delamarche, E., *Biosens. Bioelectron.* 2004, *19*, 1193–1202.

[12] Yakovleva, J., Davidsson, R., Lobanova, A., Bengtsson, M. *et al.*, *Anal. Chem.* 2004, *74*, 2994–3004.

[13] Chandrasekaran, A., Acharya, A., You, J. L., Soo, K. Y. *et al.*, *Sensors* 2007, *7*, 1901–1915.

[14] Wang, Z. H., Meng, Y. H., Ying, P. Q., Qi, C., Jin, G., *Electrophoresis* 2006, *27*, 4078–4085.

[15] Misiakos, K., Kakabakos, S. E., Petrou, P. S., Ruf, H. H., *Anal. Chem.* 2004, *76*, 1366–1373.

[16] Delamarche, E., Bernard, A., Schmid, H., Michel, B., Biebuyck, H., *Science* 1997, *276*, 779–781.

[17] Eteshola, E., Balberg, M., *Biomed. Microdevices* 2004, *6*, 7–9.

[18] Phillips, K. S., Cheng, Q., *Anal. Chem.* 2005, *77*, 327–334.

[19] Piyasena, M. E., Buranda, T., Wu, Y., Huang, J. *et al.*, *Anal. Chem.* 2004, *76*, 6266–6273.

[20] Kanda, V., Kariuki, J. K., Harrison, D. J., McDermott, M. T., *Anal. Chem.* 2004, *76*, 7257–7262.

[21] Sia, S. K., Linder, V., Parviz, B. A., Siegel, A., Whitesides, G. M., *Angew. Chem. Int. Ed.* 2004, *43*, 498–502.

[22] Jiang, X., Ng, J. M. K., Stroock, A. D., Dertinger, S. K. W., Whitesides, G. M., *J. Am. Chem. Soc.* 2003, *125*, 5294–5295.

[23] Herrmann, M., Veres, T., Tabrizian, M., *Lab Chip* 2006, *6*, 555–560.

[24] Herrmann, M., Roy, E., Veres, T., Tabrizian, M., *Lab Chip* 2007, *7*, 1546–1552.

[25] Kurita, R., Yokota, Y., Sato, Y., Mizutani, F., Niwa, O., *Anal. Chem.* 2006, *78*, 5525–5531.

[26] Liu, Y. J., Guo, S. S., Zhang, Z. L., Huang, W. H. *et al.*, *J. Appl. Phys.* 2007, *102*, 084911-1–084911-6.

[27] Sui, G., Wang, J., Lee, C. C., Lu, W. *et al.*, *Anal. Chem.* 2006, *78*, 5543–5551.

[28] Linder, V., Verpoorte, E., de Rooij, N. F., Sigrist, H., Thormann, W., *Electrophoresis* 2002, *23*, 740–749.

[29] Lin, F. Y. H., Sabri, M., Erickson, D., Alirezaie, J. *et al.*, *Analyst* 2004, *129*, 823–828.

[30] Nashida, N., Satoh, W., Fukuda, J., Suzuki, H., *Biosens. Bioelectron.* 2007, *22*, 3167–3173.

[31] Lucas, L. J., Chesler, J. N., Yoon, J. Y., *Biosens. Bioelectron.* 2007, *23*, 675–681.

[32] Murphy, B. M., He, X., Dandy, D., Henry, C. S., *Anal. Chem.* 2008, *80*, 444–450.

[33] Kim, S. H., Yang, Y., Kim, M., Nam, S. W. *et al.*, *Adv. Funct. Mater.* 2007, *17*, 3493–3498.

[34] Bai, Y., Koh, C. G., Boreman, M., Juang, Y. J. *et al.*, *Langmuir* 2006, *22*, 9458–9467.

[35] Nelson, K. E., Foley, J. O., Yager, P., *Anal. Chem.* 2007, *79*, 3542–3548.

[36] Pugia, M. J., Blankenstein, G., Peters, R. P., Profitt, J. A. *et al.*, *Clin. Chem.* 2005, *51*, 1923–1932.

[37] Bhattacharyya, A., Klapperich, C. M., *Biomed. Microdevices* 2006, *9*, 245–251.

[38] Liang, K., Mu, W., Huang, M., Yu, Z., Lai, Q., *Biomed. Microdevices* 2007, *9*, 325–333.

[39] Honda, N., Linberg, U., Andersson, P., Hoffmann, S., Takei, H., *Clin. Chem.* 2005, *51*, 1955–1961.

[40] Mulvaney, S. P., Cole, C. L., Kniller, M. D., Malito, M. *et al.*, *Biosens. Bioelectron.* 2007, *23*, 191–200.

[41] Dong, H., Li, C. M., Zhang, Y. F., Cao, X. D., Gan, Y., *Lab Chip* 2007, *7*, 1752–1758.

[42] Kartalov, E. P., Zhong, J. F., Scherer, A., Quake, S. R. *et al.*, *BioTechniques* 2006, *40*, 85–90.

[43] Kartalov, E. P., Anderson, W. F., Scherer, A., *J. Nanosci. Nanotechnol.* 2006, *6*, 2265–2277.

[44] Unger, M. A., Chou, H.-P., Thorsen, T., Scherer, A., Quake, S. R., *Science* 2000, *288*, 113–116.

[45] Hansen, C. L., Sommer, M. O. A., Quake, S. R., *Proc. Natl. Acad. Sci. USA* 2004, *101*, 14431–14436.

[46] Kartalov, E. P., Walker, C., Taylor, C. R., Anderson, W. F., Scherer, A., *Proc. Natl. Acad. Sci. USA* 2006, *103*, 12280–12284.

